IMPROVEMENT OF A WIGGLER BY SINGLE AXIS MAGNETIC MEASUREMENT, VIRTUAL SYNTHESIS, AND RELOCATION OF MAGNETS

H. S. Marks*, M. Volshonok, E. Dyunin, A. Gover, Tel Aviv University
Y. Lasser, R. Shershevski, A. Yahalom, Ariel University Centre

ABSTRACT

Deviations in the electron beam trajectory through the planar wiggler of the Israeli Electrostatic Accelerator FEL were found to be primarily caused by small variations in the strength and angle of polarisation of lateral focussing bar magnets which are positioned on both sides of the wiggler, and provide a quadrupole guiding field on axis.
The field of the wiggler on axis was measured using a Labview controlled automated system built in our lab, based on a 2-axis Hall Effect magnetic sensor driven by a stepper motor. Polarisation field components of the individual focussing magnets were measured separately. Then, using an algorithm, the focussing magnets were paired, such that their non-uniformities were utilised to not only cancel out each other's error, but also to cancel out the field errors on axis due to variation in strength and polarisation angle of the wiggler magnets.

The quality of the predicted electron beam transport was evaluated by 3-D simulation with the General Particle Tracer code which allowed the input of all the measured fields.

INTRODUCTION

Free electron lasers are devices that transform the kinetic energy of electrons into electromagnetic radiation. They can operate with a wide range of frequencies, exhibiting high power, high efficiency, and tunability [1]. The work described in this article was on the Wiggler of an electrostatic accelerator free electron laser (EA FEL). The Wiggler is a magnetic cavity which causes injected electrons to oscillate as they pass through. This oscillation generates radiation, which due to the relativistic speed of the electrons is primarily focussed in the direction of electron travel.

Various schemes have been proposed for the optimisation of wigglers with fixed magnets [2], [3], [4], [5]. The optimisations are typically required due to imperfect alignment of the polarisation fields of the magnets together with differences in field strengths between magnets.

The Wiggler which is the subject of this work is 1.201m long and is comprised of an entrance section to place the electrons in the correct wiggling trajectory, 26 magnetic periods of length 44.44 mm for the wiggling, and finally an exit section so the electrons leave the wiggler along the central axis. The periods are arranged in a Halbach planar configuration.

As part of a series of recent upgrades to the Israeli EA FEL, measurements were made of the planar Wiggler with the intention of using these measurements to better model electron transport. The average peak amplitude of the principal field along the central axis was 1.93kG with a standard deviation of ±54G.

For lateral focussing 23 magnets of length 50.8 mm were placed along the length of the Wiggler on either side to provide a guiding quadrupole field (see fig 1), gaps between these magnets were filled with Teflon spacers of width ~1.4 mm. The magnetic fields in the transverse x-y directions were measured along 5-axes using a Hall Probe (F.W. Bell 9950 YOB-25) These axes were at x=y=0mm from the centre of the wigglers mechanical/geometrical axis, x=±4, y =0mm and x=0, y =±4mm. The probe was moved forward in steps of 1mm using a stepper motor. At each step a reading was taken and recorded using a data acquisition card and Labview software. The measurements showed non-uniformities in the lateral focussing field of up to 50G.

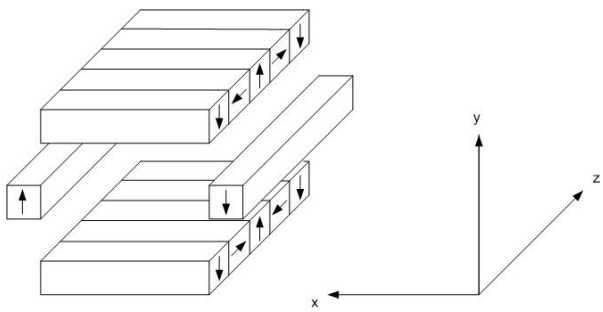

Figure 1: Diagram showing the relative positions of the principal and lateral magnets within the wiggler.

The lateral focussing magnets were then removed from the Wiggler and readings taken of the fields along 5 axes. These readings were more uniform which demonstrated that the perturbations were principally from the longitudinal magnets, nevertheless, deviations of up to 20 Gauss were still present along the central axis. Ideally there would be no Bx field from the focussing magnets at the side and less variation in the strength of the principal field (By), however, due to imperfect manufacture this was not the case.

The measurements off the central axis where used to confirm the model of the magnetic field [6] which was inserted into the General Particle Tracer (GPT) code. The

* Corresponding author. Email: harry@eng.tau.ac.il

model for the Wiggler magnets used which satisfied $\nabla \cdot B = 0$ and $\nabla \times B = 0$ is:

$$B_y^W(y,z) = B_0^W \cos(k_\omega z)\cosh(k_\omega y)\hat{y} \quad (1)$$

$$B_z^W(y,z) = -B_0^W \sin(k_\omega z)\sinh(k_\omega y)\hat{z} \quad (2)$$

Using the measured data of $B_y(0,z)$ (on axis as a function of z), equations (1) and (2) are inserted into GPT in the form of (3) and (4):

$$B_y^W(y,z) = B_y(z)\cosh(k_\omega y)\hat{y} \quad (3)$$

$$B_z^W(y,z) = \frac{\partial B_y}{\partial z}\frac{\tanh(k_\omega y)}{k_\omega}\hat{z} \quad (4)$$

Consider the Lorentz force equation:

$$F = -e\begin{pmatrix} \hat{x}[v_y \frac{\partial B_y}{\partial z}\frac{\tanh(k_\omega y)}{k_\omega} - v_z B_y(z)\cosh(k_\omega y)] \\ -\hat{y}[v_x \frac{\partial B_y}{\partial z}\frac{\tanh(k_\omega y)}{k_\omega} - v_z B_x] \\ +\hat{z}[v_x B_y(z)\cosh(k_\omega y) - v_y B_x] \end{pmatrix} \quad (5)$$

A perfectly centred electron beam entering an ideal planar wiggler in which $B_x = 0$ will undergo betatron oscillation in the y direction due to the finite radius of the beam (as at $|y| > 0$, $|B_z| > 0$). In our real case the force in the y direction is either damped or amplified by the contribution of Bx. This growth in v_y interferes with the forces in the x-z plane, disturbing the electron trajectories. We avoided disassembly of the wiggler magnets, and relied only on replacement and re-pairing of the lateral focusing magnets in order to improve the wiggler trajectories. The lateral focusing magnets could be arranged such that not only would the B_x perturbations be minimised but also the betatron oscillations damped.

The strengths of individual lateral focusing magnets were measured using a jig which held the magnets at the same distance from the probe as the magnets would be from the central axis of the Wiggler. The magnets B_x and B_y components were measured and used in the pairing algorithm described in the next section.

METHOD OF REPAIR

The algorithm for improving the fields incorporated the following steps. First the measured on-axis $B_y(z)$ and $B_x(z)$ data was interpolated using a cubic spline into intervals of 0.1mm from intervals of 1mm. The $B_y(z)$ and $B_x(z)$ fields were measured with all magnets in place, and then with the lateral focussing magnets removed.

The $B_x(z)$ data needed to be filtered to remove the periodic components of the principal $B_y(z)$ field which would be measured due to the difficulty of perfectly aligning the probe. The $B_y(z)$ data was filtered in order to see the background perturbations to the sinusoidal field. To filter, the integral of the field at each point along the z-aixs was taken from $z - \lambda_W/2$ to $z + \lambda_W/2$, where λ_W is the wiggler period (44.44mm).

Previously there were 23 lateral focussing magnets of average strength 9.5kG on each side of the wiggler. Whilst this arrangement provided strong focussing in the x-z plane, it reduced the focussing effect in the y-z plane of the principal wiggler magnets. It was calculated that 17 equally-spaced magnets of an available set of average strength 8.1kG would provide optimal lateral and vertical focusing along the wiggler and the best [x(0), x'(0), y(0), y"(0)] phase space acceptance at the entrance to the wiggler.

In order to deal with the background perturbation fields the filtered data of the fields along the length of the wiggler was divided into seventeen sections of length 71.8mm, corresponding to the proposed introduction of the 17 focussing magnets. The average background field in each of the 17 regions was determined by summation of the interpolated filtered data. This was not done for the data in the first and last regions at the start and end of the wiggler as the fields were not sinusoidal, these regions were treated separately.

The results of the averaging for each region were stored in separate 1D matrices, one for B_x and one for B_y. From a list of all the available magnets, the lateral focussing magnets in use and other spare magnets, two 1D matrices of their By and Bx values were formed.

The procedure used for choosing the best pair of magnets required that their combination would minimise the perturbation field within a particular region. The first step was to find the pairs that minimised the Bx field, then the pairs that minimised By, and finally which combinations would minimise the perturbations to both axes.

A square matrix was formed of the sums and differences of the Bx fields of the magnets:

$$\mathbf{Bx}_{m,n} = (1-\delta_{mn})\left\|Bx_n\right| + \mathrm{sgn}(m-n)\left|Bx_m\right\| \quad (6)$$

This matrix describes all the possible arrangements of Bx. The matrix for the By values was simpler:

$$\mathbf{By}_{m,n} = \left|By_n - By_m\right| \quad (7)$$

This was because the orientations in which the By field could be placed were limited by the wiggler setup which called for the longitudinal magnets on the left side to be pointing in the +Y direction and the magnets on the right side to be pointing in the –Y direction such that the By field on axis cancelled.

As there were 66 possible lateral focusing magnets, two 66*66 matrices were formed from equations (6) and (7). The pairing for the 1st and 17th position was left till last. Each of the pairs for the intervening sections was chosen using the following procedure.

The B_x and B_y background of each of the sections was subtracted from each of the matrix elements of equation (6) and (7) respectively, resulting in two new matrices for each of the seventeen sections. The minimum value in each matrix represented the best combination for either the B_x or B_y axis. Equal weight is given to the importance of minimising the perturbations to the B_x and B_y fields.

The two new matrices for each section were then added and the location of the minimum value of the resultant matrix for each section informed us which pair of magnets minimises the perturbations (in that region). The m^{th} and n^{th} row of the matrix represented the m^{th} and n^{th} values of the 66*1 matrix which was the list of the available magnets. The field at the entrance and exit to the wiggler, the 1^{st} and 17^{th} position were not amenable to the same treatment. Whilst it was desirable to minimise B_x at the entrance, at the end it was desirable to use small B_x components to correct any angular deviation of the beam leaving the wiggler (likewise for the B_y components at the end of the wiggler). The B_y components at the entrance had to be chosen such that the electron was deflected into the correct undulating trajectory.

In order to evaluate the repair of the wiggler the B_x and B_y fields on axis were re-measured after the lateral focussing magnets had been re-arranged according to the results of the algorithm. The data was then inserted into GPT. In our GPT model the lateral magnets were programmed in separately from the principal field due to their different position. The field measured on axis after the repair included the field of lateral magnets. To avoid duplicating the field of the lateral magnets using GPT the field of the lateral magnets on axis was deducted from the measured data on axis so that the simulated lateral magnets could then be programmed in (as each of the individual lateral magnets had been measured separately).

RESULTS

The results of the repair can be most clearly illustrated by plotting the Bx of the field on axis before and after the repair (figure 2). The Maximum deviation of the Bx field after the optimisation is 0.5% of the principal field along the central axis.

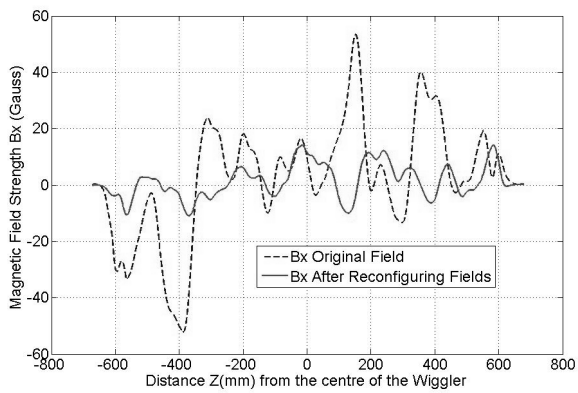

Figure 2: Bx measured along the central axis before and after optimisation.

Figures 3 and 4 show the GPT simulation results of the electron beam propagation through the wiggler using the fields measured after the optimisation of the magnets. Figure 3 shows propagation in the x-z plane with some betatron oscillation, whilst in figure 4 both scalloping and betatron oscillations are present. The electron beam parameters such as the wiggling amplitude and beam diameter are similar to that simulated for an ideal wiggler with space charge. The beam shown in figures 3 & 4 consists of 25 cells representing a total current of 1.75 A. The space available to the electron beam is (the size of the waveguide) ±7.5 mm in the x-z plane and ±5.35 mm in y-z plane.

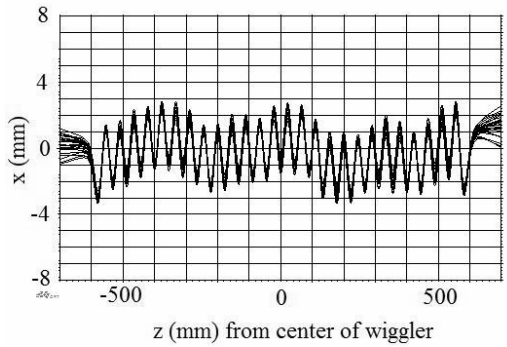

Figure 3: The trajectory in the x-z plane of an electron beam passing through the wiggler.

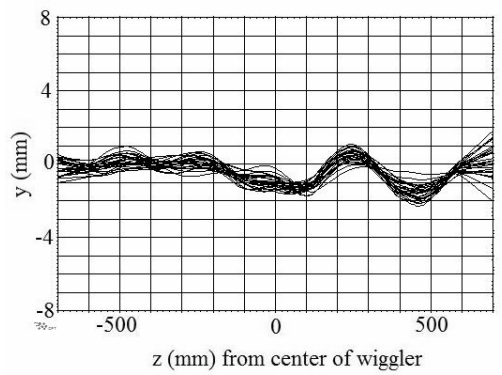

Figure 4: The trajectory in the y-z plane of an electron beam passing through the wiggler.

DISCUSSION

The extent of field optimisation was limited by the uncertainty of the exact position of the probe within the wiggler. The probe sat within a metal block which was moved along the inside of the wiggler. The outer dimensions of the block were slightly smaller than that of the wiggler in order to allow it to pass through, whilst the probe was positioned at the centre of the block. To compensate for the uncertainty of the position of the block within the wiggler and that of the position of the hole in the centre of the block each field was measured four ways, with the block and wiggler in different orientations about the z-axis. These measurements were averaged to determine the field along the central axis. However, the uncertainty in this method prevented the field being improved much beyond that shown in figure 2.

CONCLUSION

We have demonstrated that it is possible to ameliorate the effect of field aberrations caused by variations in field strength and polarisation of the main wiggler magnets by selecting appropriate magnets for the guiding quadrupole field and pairing them optimally. The selection is achieved using an algorithm which is not computationally demanding. We suggest this method as a simple scheme for providing lateral focusing in linear wigglers in general, and for improving the transport parameters of imperfect wigglers.

ACKNOWLEDGEMENT

We thank S.B. van der Geer and M.J. de Loos of Pulsar Physics for programming assistance with GPT. And we thank Joachim Pflueger from DESY for his advice on magnets.

REFERENCES

[1] A. Gover, "Laser: Free Election Lasers", Encyclopedia of Modern Optics, Elsevier, 2005.

[2] J.N. Ortega, C. Bazin, and D.A.G. Deacon, "Optimization of a permanent magnet undulator for free electron laser studies on the ACO storage ring", Journal of Applied Physics 54(9), pp 4776-4783, Sept. 1983

[3] R.A. Cover, B.L. Bobbs, G. Rakowsky, M.M. Johnson, and S.P. Mills, "FEL Performance with Pure Permanent-Magnet Undulators having Optimised Ordering", Nuclear Instruments and Methods in Physics Research A296 (1990) 603-606

[4] B Diviacco, R.P. Walker, "Recent advances in undulator performance optimization", Nuclear Instruments and Methods in Physics Research A 368 (1996) 522-532.

[5] R. Hajima, F. Matsuura, "Advanced Optimization of permanent magnet wigglers using genetic algorithm", Nuclear Instruments and Methods in Physics Research A 375 (1996)

[6] A. Gover, H. Freund, V. H. Granatstein, J. H. Mc Adoo, and Chai-Mei Tang, Infrared and Millimeter Wave, Vol. II, Chapter 8, "Design Considerations for Free Electron Lasers Driven by Electron Beams from RF Accelerators", Ed. K. Button, Academic Press, 1984.